Journal of Materials Chemistry C

Using Ultra-Fast Spectroscopy to Probe the Excited State Dynamics of a Reported Highly Efficient Thermally Activated Delayed Fluorescence Chromophore

Journal:	*Journal of Materials Chemistry C*
Manuscript ID	TC-ART-11-2018-005957.R2
Article Type:	Paper
Date Submitted by the Author:	08-Feb-2019
Complete List of Authors:	Vázquez, Ricardo J.; University of Michigan Kim, Hyungjun; Incheon National University, Chemistry Zimmerman, Paul; University of Michigan, Chemistry Goodson, Theodore; University of Michigan, Department of Chemistry

Using Ultra-Fast Spectroscopy to Probe the Excited State Dynamics of a Reported Highly Efficient Thermally Activated Delayed Fluorescence Chromophore.

Ricardo Javier Vázquez [a], Hyungjun Kim [b], Paul M. Zimmerman [a], and Theodore Goodson III [a,*]

[a] Department of Chemistry, University of Michigan, Ann Arbor, MI 48109

[b] Department of Chemistry, Incheon National University, Incheon 22012, Republic of Korea

***Corresponding Author**: tgoodson@umich.edu

Associated Content

Electronic supplementary information (ESI) available

ABSTRACT

Multiple ultrafast spectroscopic techniques and quantum chemical simulations (QCS) were used to investigate the excited state dynamics of BCC-TPTA. This organic chromophore is believed to possess excited state dynamics governed by a thermally activated delayed fluorescence (TADF) mechanism with a reported internal quantum efficiency (η_{IQE}) of 84 %. In addition, a significant enhancement in its quantum yield ($\boldsymbol{\Phi}$) in solution after purging oxygen has been reported. This $\boldsymbol{\Phi}$ enhancement has been widely accepted as due to a delayed fluorescence process occurring in the μs time-scale. The spectroscopic measurements were carried out both in solution and blended films, and from *fs* to μs time-scales. The excited state dynamics of Rhodamine B and $Ir(BT)_2(acac)$ were also probed for comparison. Investigations in the absence of oxygen were also carried out. Our time-correlated single photon counting (TCSPC) measurements revealed a lack of long-lived emissive lifetime for BCC-TPTA in any of the medium tested. Our *ns* transient absorption spectroscopy (*ns* TAS) experiments revealed that BCC-TPTA does not possess triplet transient states that could be linked to a delayed fluorescence process. Instead, the evidence obtained from our spectroscopic tools suggest that BCC-TPTA has excited state dynamics that of a typical fluorescence chromophore and that just comparing the $\boldsymbol{\Phi}$ difference before and after purging oxygen from the solution is not an accurate method to claim excited state dynamics governed by a delayed fluorescence mechanism. Consequently, we believe that previous studies, in which the photo-physics of organic chromophores with TADF characteristics are reported, may have overlooked the influence of the host materials on the obtained optical properties in blended films.

Keywords: TADF, OLED, reverse intersystem crossing, dynamic equilibrium, excited-state dynamics, and ultrafast spectroscopy.

1. INTRODUCTION

There is still a great need for more efficient green and blue organic materials for light emitting diode (OLEDs) applications.[1,2] While phosphorescent materials have shown some success, their short lived lifetimes, high cost, and poor stability, impart several limitations.[3,4] The thermally activated delayed fluorescence (TADF) mechanism has been proposed as a cost-efficient alternative to get higher efficiencies and longer device lifetimes and there has been great success regarding the synthesis of novel TADF chromophores. Some of these materials have reported internal quantum efficiency (η_{IQE}) values approaching 100 %.[2,5–7] This very high internal quantum efficiency was suggested as due to the harvesting of triplets in the chromophore in a reverse intersystem crossing process (rISC).[3,8–10] Unfortunately, the high turnover of new TADF scaffolds has not allowed for the necessary and intricate spectroscopic measurements for each new molecule to be elucidated individually in order to fully understand the mechanism. The previous reports have utilized primarily steady-state and *μs* spectroscopy to illustrate the thermally activated rISC process,[11] however, these time-resolved measurements can be convoluted with the parallel existing phosphorescence in the chromophore.[2,6,11] One of the best TADF chromophores, 9'-[4-(4,6-diphenyl-1,3,5-triazin-2-yl)phenyl]-9,3':6',9''-ter-9H-carbazole (BCC-TPTA), was reported to have an η_{IQE} of ~ 84 %.[2] This material is believed to represent the basic motif of an impressive TADF system and its efficiency sets a standard as to what other materials seek to attain. However, the details of its excited state dynamics have not been elucidated with the proper spectroscopic tools.

One way to characterize the contribution between singlet or triplet emission is to carry out time-resolved measurements with the appropriate time-resolution, as well as oxygen quenching measurements to distinguish between the contributions of the singlet and triplet emission.[6,12–14] It

is interesting to note that while there have been reports of studies investigating the emission of highly efficient and very well-known TADF structures, there have not been any detailed time-resolved fluorescence and time-resolved fluorescence lifetime quenching studies of these promising materials.[15] Moreover, many previous studies were conducted in the solid state using TADF chromophores as the guest material in blended films. Recent publications have highlighted the potential influence of exciplex formation of the guest, and between the host and the guest materials (host:guest) on the obtained solid state photoluminescence decay lifetime of chromophores with TADF charasteristics.[16–19] Aditionally, the steady state optical properties of the most common materials used as hosts overlaps with ones of the materials used as guests, which could give rise to Föster resonance energy transfer (FRET) and Dexter energy transfer (DET) mechanisms among the chromophores.[18,19] Therefore, optically inert hosts should be used to elucidate the photoluminescence decay lifetime and excited state dynamics in film of chromophores with TADF character.

In this report, ultrafast spectroscopic methods, with an emphasis in the *ns* TAS, are coupled with quantum chemical simulations (QCS) to elucidate the excited state dynamics in the well-known BCC-TPTA chromophore. For the measurements conducted in film, we selected poly methyl methacrylate (PMMA) as the host material. PMMA possess high transmission properties in the range of wavelengths used in this study and is also highly impermeable to oxygen.[20] Specifically, PMMA is optically inert, and cannot be excited by any of the excitation wavelengths used in this study, unlike most of the common hosts used in previous studies.[18,19,21] This prevented any convolution between the host and the guests excited state dynamics. In addition, previous studies conducted with similar organic chromophores with TADF characteristics doped in PMMA films have reported emissive lifetimes in the μs regime. The long-lived emissive lifetime in these

chromophores has been ascribed to a delayed fluorescence process.[15,19] As a comparison, we investigated a metal-containing primary phosphorescence chromophore $Ir(BT)_2(acac)$ and a well-known fluorescence chromophore Rhodamine B. Also, we investigated the emissive dynamics of these systems in a range of temperatures after purging oxygen from the solution by N_2 bubbling.

2. EXPERIMENTAL SECTION

2.1 ***Steady State Measurements:*** The absorption spectra were measured on an Agilent 8341 spectrophotometer. The emission spectra were collected on a Fluoromax-4 fluorimeter with slits set at 1 nm and an integration time of 0.100 s. Quartz cells with 10 mm path lengths were used for all the steady-state measurements. All optical measurements were carried out at ambient conditions. The fluorescence quantum yields ($\boldsymbol{\Phi}$) measurements were conducted by using the Williams comparative method. The optical density was set to be ~ 0.10 or below to avoid reabsorption and internal filter effects. The absorption and fluorescence were measured for four samples with decreasing concentrations. The $\boldsymbol{\Phi}$ for BCC-TPTA dissolved in toluene and for Ir(BT)2(acac) dissolved in THF were measured using Coumarin 30 ($\boldsymbol{\Phi}$ = 0.67)[22] dissolved in acetonitrile as the standard. The same is true for the $\boldsymbol{\Phi}$ measurements after purging out oxygen (10 minutes). Rhodamine B is a well-known standard and the $\boldsymbol{\Phi}$ value can be found elsewhere. The $\boldsymbol{\Phi}$ of Rhodamine B after purging out oxygen (10 minutes) were measured as well and compared to itself ($\boldsymbol{\Phi}$ = 0.67)[23] before purging. The low temperature emission (phosphorescence) spectrum were obtained by using a Photon Technologies International (PTI), QuantaMaster 400 scanning spectrofluorimeter. The emission spectrum of the samples at low temperature (77K) were obtained after a delay of $> 100\ \mu s$ between the excitation beam and emission detection.

2.2 Time-Resolved Fluorescence and Phosphorescence Measurements: *The ultra-fast fluorescence upconversion (UpC)* setup was used to measure the fluorescence with *ps* time resolution as it has been previously described.[14] A mode-locked Ti-sapphire femtosecond laser (Spectra-Physics Tsunami) was used to generate 80 fs pulses at 800 nm with a repetition rate of 82 MHz. This Ti-sapphire mode-locked laser was pumped by a 532 nm CW laser (Spectra-Physics Millennia), which has a gain medium of neodymium-doped yttrium vanadate (Nd:YVO4). After the 800 nm pulsed beam is generated, a second harmonic (β- barium borate crystal) generates a 400 nm excitation pulse. The residual 800 nm beam was directed to pass through a computer-controlled motorized optical delay line. A Berek compensator controlled the polarization of the 800 nm excitation beam power varied between 33 to 40 mW. The fluorescence emitted by the sample was upconverted by the residual 800 nm beam by a nonlinear crystal of β-barium borate. It is important to mention that the 800 nm beam is passed by the optical delay line with a minimum gate step of 6.25 fs. The monochromator is used to select the wavelength of the up-converted beam of interest, and the selected beam is detected by a photomultiplier tube (R152P, Hamamatsu, Hamamatsu City, Japan). The photomultiplier tube (PMT) converts the detected beam into photon counts, which can be read from a computer. Coumarin 30 was used for calibrating the laser for the range of emission wavelengths in this study. The instrument response function (IRF) has been determined from the Raman signal of water to have a width of 110 fs.[24] Lifetimes of fluorescence decay were obtained by fitting the fluorescence decay profile to the most accurate fit. *The time-correlated single photon counting (TCSPC)* technique, which has been described previously,[14] was used to study the fluorescence and phosphorescence of the investigated chromophores. The laser used for the TCSPC measurement was a Kapteyn Murnane (KM) mode-locked Ti-sapphire laser. The output beam from the KM laser was at 800 nm wavelength has a pulse duration of ∼30 fs.

The 800 nm output beam was frequency-doubled using a nonlinear barium borate crystal to obtain a 400 nm beam. Focus on the sample cell (quartz cuvette, 0.4 cm path length) was ensured using a lens of focal length 11.5 cm. Collection of fluorescence was done in a direction perpendicular to the incident beam into a monochromator, and the output from the monochromator was coupled to a photomultiplier tube, which converted the photons into electrical signals (counts). The Time Harp 200 is the PCI-board in charge of the histogram of photon creation (65,000 max) and its subsequent conversion into electrical signals. This electronic conversion process allows other electronic equipment in the room to interfere with the detection if the histograms are not finished fast enough. Therefore, electronic interference could be detected depending on how much time it takes to create the histogram (collect the 65,000 photons). The high density of photons by the excitation source make the IRF detection fast enough so no electronic interference is detected. In contrast to the IRF detection, the histogram created for the investigated samples are usually significantly slower than for the IRF.

2.3 Nanosecond Transient Absorption Spectroscopy Measurements*:* The absorption and lifetime of emissive and non-emissive transient species can be probed by using transient absorption spectroscopy, which has been previously described.[25,26] These measurements were done in diluted solutions and in the same solvents in which the other photophysical characterization were carried out. A LP980 (Edinburgh) system, which contains the photomultiplier (PMT-LP), was coupled with a Spectra-Physics QuantaRay Nd:YAG nanosecond (*ns*) pulsed laser and a GWU Optical Parametric Oscillator (OPO) tunable from 250 nm to 2600 nm for the excitation source. For this investigation, a 415 nm excitation beam was used to pump the molecules and a pulsed xenon lamp white light continuum was used for probing the excited state.

2.4 Quantum Chemical Simulation: The ground state (S_0) geometries of BCC-TPTA and Rhodamine B were optimized using density functional theory (DFT). The B3LYP functional, which has successfully predicted the ΔE_{ST} of a variety of TADF materials, was used along with the 6-31G* basis set.[2] The first excited singlet state (S_1) geometry of BCC-TPTA was obtained with a restricted open-shell Kohn-Sham (ROKS) approach and 6-31G* basis sets. ROKS is known to improve the deficiency of semilocal linear response time-dependent DFT (LR−TD−DFT) and offers a good alternative for investigating charge transfer states.[27–31] Rhodamine B is a symmetric molecule and has a positive unit charge on one nitrogen atom. Due to a closed manifold of low lying states, however, excited state geometry optimization of Rhodamine B using TDDFT and ROKS did not easily lead to a symmetry broken state. Therefore, S_1 of Rhodamine B was targeted using configuration interaction single (CIS) geometry optimization, which had no issue distinguishing the two states. The single point energy of S_1 is refined using TD-DFT based on ROKS BCC-TPTA geometry and CIS Rhodamine B geometry.

The first triplet (T_1) geometry was predicted with spin unrestricted DFT. Single point energy calculations to evaluate the fluorescence emission energies, spin−orbit coupling elements, and adiabatic energy gap ($\Delta E_{ST} = E_{\text{TDDFT } S1 \text{ at min } S1} - E_{\text{UDFT } T1 \text{ at min } T1}$) were conducted, and the solvent environment effect is treated using a polarizable continuum model. The dielectric constant of chloroform and ethanol of 4.31 and 24.3 is used to describe the solvent medium of BCC-TPTA solution and Rhodamine B solution, respectively. All quantum chemical calculations were performed using Q−Chem 5.0.[32] The rate constant of ISC and rISC, were estimated via Fermi's Golden rule,[33,34]

$$k_{\text{ISC}} = \frac{2\pi}{\hbar}\rho_{\text{FC}}|\langle S_1|H_{SO}|T_1\rangle|^2$$

where $\langle S_1|H_{SO}|T_1\rangle$ is the spin−orbit coupling element between S_1 and T_1, ρ_{FC} denotes the Franck−Condon weighted density of states, and $\hbar$ is the reduced Planck constant of 6.582×10^{-16} eVs. ρ_{FC} is evaluated with Marcus−Levich−Jortner theory, [35,36]

$$\rho_{FC} = \frac{1}{\sqrt{4\pi\lambda_M k_B T}} \sum_{n=0}^{\infty} \exp(-S)\frac{S^n}{n!} \exp[-\frac{(\Delta E_{ST} + n\hbar\omega_{eff} + \lambda_M)^2}{4\pi\lambda_M k_B T}]$$

where λ_M is the Marcus reorganization energy associated with the intermolecular and intramolecular low−frequency vibrations, k_B is for Boltzmann constant of 8.6173×10^{-5} eV/K, T is the temperature (in this study, 298.15 K), $\hbar\omega_{eff}$ represents the effective energy of a mode representing the nonclassical high−frequency intramolecular vibrations. Huang−Rhys factor associated with these modes are given as *S*. The rate constant of the rISC process was described by parameters generated at the T_1 geometry, and the k_{ISC} estimation with parameters relevant to the S_1 geometry.

One recent computational study on TADF mechanism discussed the rate of rISC within the same framework used in this work. They computed the contribution of non-classical intramolecular vibrations and estimated the Marcus reorganization energy due to low frequency intramolecular vibrations and the medium-induced relaxation effects to be in the range of ~0.1-0.2 eV.[36–38] Also, they assumed the Huang-Rhys factors can be neglected without significant changes to the results for large molecules. The approximation setting λ_M to 0.1 or 0.2 eV reproduced available experimental k_{RISC} values on the same order of magnitude. The close examination revealed that use λ_M value of 0.2 eV gave better quantitative agreement with the available experimental k_{RISC} dta. Therefore, λ_M value is set to 0.2 eV in this study.

The fluorescence emission rate (k_F) was approximated by the product of the oscillator strength and the square of the wavenumber.[39] The observed k_F values of anthraquinone-based

intramolecular charge transfer compounds, one class of TADF materials reported by the Adachi group, could be reproduced with this simple calculation.[39]

3. RESULTS

3.1 Steady-State Measurements: UV-Vis Absorption. The UV-Vis (steady-state absorption) spectra at ambient conditions for Rhodamine B, $Ir(BT)_2(acac)$, and BCC-TPTA were taken in a diluted solution of ethanol, tetrahydrofuran (THF), and toluene, respectively. Their absorption spectra are shown in ***Figure 1B*** and data is summarized in ***Table 1***. All of the investigated chromophores absorb in the visible region. The absorption spectra of Rhodamine B is perfectly in agreement with what is previously reported in the literature as well as is the absorption spectra of the $Ir(BT)_2(acac)$ complex.[40,41] For BCC-TPTA, two main absorption bands are present as is typical for chromophores with donor-acceptor configuration.[14] The high-energy band (<300 nm) is attributed to the localized excitations of the chromophore, while the lower energy band (300-400 nm) is consistence with absorption of the charge transfer state of BCC-TPTA.[14]

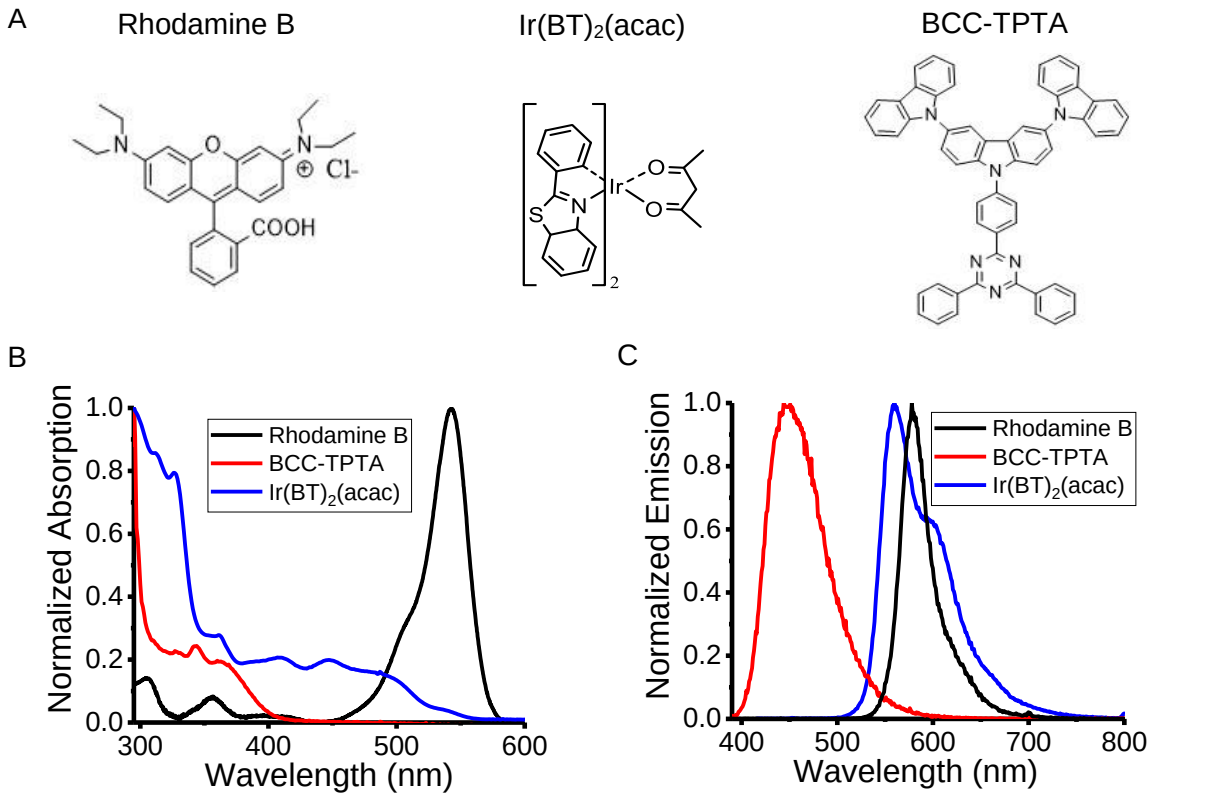

Figure 1. (A) Molecular structure of the investigated chromophores; steady-state absorption (B) and emission (C) of the investigated chromophores. All measurements were carried out in solution.

3.2 Steady-State Measurements: Fluorescence and Phosphorescence Spectra. The emission spectrum under ambient conditions of Rhodamine B, $Ir(BT)_2(acac)$, and BCC-TPTA were taken in diluted solutions of ethanol, tetrahydrofuran (THF), and toluene, respectively. The emission spectra are shown in ***Figure 1C*** while the data is summarized in ***Table 1.*** All of the investigated chromophores emit in the visible region and their emission spectra are in agreement with the ones previously reported in the literature. The quantum yield (***Φ***) of the investigated chromophores was measured before and after the oxygen purging process (***Table 1***). This allowed us to evaluate the potential contribution from the triplet state to the emissive characteristics of the investigated chromophores. There was a very small difference in the ***Φ*** of Rhodamine B after the solution was purged of oxygen (67 % to 69 %) that is within the margin of error for the Williams method.[42] As

expected for phosphorescence chromophores, the ***Φ*** measured for the $Ir(BT)_2(acac)$ complex increased from 1% to 15 % after oxygen purging.[11,43] For BCC-TPTA, our measurements showed a 15 % ***Φ*** enhancement (from 58 % to 67 %) after the solution was purged of oxygen. This ***Φ*** enhancement after the oxygen purging process has been widely ascribed to a delayed fluorescence process occurring somewhere in the *μs* timescale.[2,6,15]

Moreover, we investigated the influence of the temperature and the solvent polarity on the emission spectra of BCC-TPTA. As can be observed in ***Figure S1***, the emission intensity of BCC-TPTA is inverse proportional to the temperature. Similar behavior was obtained for Rhodamine B and for the $Ir(BT)_2(acac)$ complex. According to the Lippert-Mataga model, the charge transfer character of emitting species can be probed by evaluating how the emission λ_{max} changes due to solvent polarity (*f*).[44,45] As could be observed from the plot of the Stokes shift ($\nu_a - \nu_f$) in function of the (*f*), we obtained a linear relationship between $\nu_a - \nu_f$ and *f* with a large slope of 15,360 cm^{-1} (***Figure S14***). This implies that the emission dynamics of BCC-TPTA is highly sensitive to the solvent polarity while its absorption spectra is unaffected. The large slope obtained from the Lippert-Mataga model correlates well with the charge transfer state assignment from the steady state absorption of BCC-TPTA (***Figure 1B***). Therefore, we can rule out the possibility of any exciplex formations in this study.

Table 1. Steady state measurements relevant data.

Chromophores	Extinction Coefficient	λ_{maxEm}	***Φ*** %	***Φ*** % Purged	ΔE_{st} (eV) Theo	ΔE_{st} (eV) Exp	Stern-Volmer Quenching Rates $M^{-1}s^{-1}$
Rhodamine B (Fluorescence)	105,000 $cm^{-1}M^{-1}$ at 545 nm	575 nm	67 [40]	69	*	*	1.4×10^{10}
$Ir(BT)_2(acac)$ (Phosphorescence)	51,000 $cm^{-1}M^{-1}$ at 328 nm	560 nm	1	15	*	*	2.31×10^{9}
BCC-TPTA (TADF)	17,362 $cm^{-1}M^{-1}$ at 342 nm	450 nm	58	67	0.114[2]	0.34	$2.82\ 10^{8}$

(*) This molecule has a $\Delta E_{st} > 0.3$ eV.

In order to evaluate the differences in energy levels between the S_1 and T_1 state (ΔE_{st}), the phosphorescence spectrum of the investigated chromophores was also probed. Their spectra are shown in ***Figure S2*** and the data is summarized in ***Table 1.*** For Rhodamine B, we were not able to get a phosphorescence spectrum at any of the concentrations tested. Likely, the phosphorescence emission of the Rhodamine B was too low to be detected.[46] A sharper emission spectrum at 77 K than the one taken at RT was obtained for the $Ir(BT)_2(acac)$ complex. This sharpening in the emission spectrum can be explained by to the lack of molecular vibrations promoted by room thermal energy.[47,48] A red-shift in the phosphorescence spectrum of BCC-TPTA at 77 K was observed relative to its fluorescence spectrum taken at the same temperature (***Figure S2***). We noticed that the fluorescence spectrum of BCC-TPTA at 77 K was blue shifted relative to the one obtained at RT (***Figure S3***). We calculated the ΔE_{st} to be 0.34 eV from the fluorescence and phosphorescence spectrums obtained at 77 K. A slightly smaller value was obtained if the fluorescence spectrum at RT was used for the calculation.[2,15] These small ΔE_{st} give hints of a potential excited state mixing between the S_1 and T_1 state, and if correct, it should be observed as long-lived emissive lifetime in the μs timescale.[6,18,19]

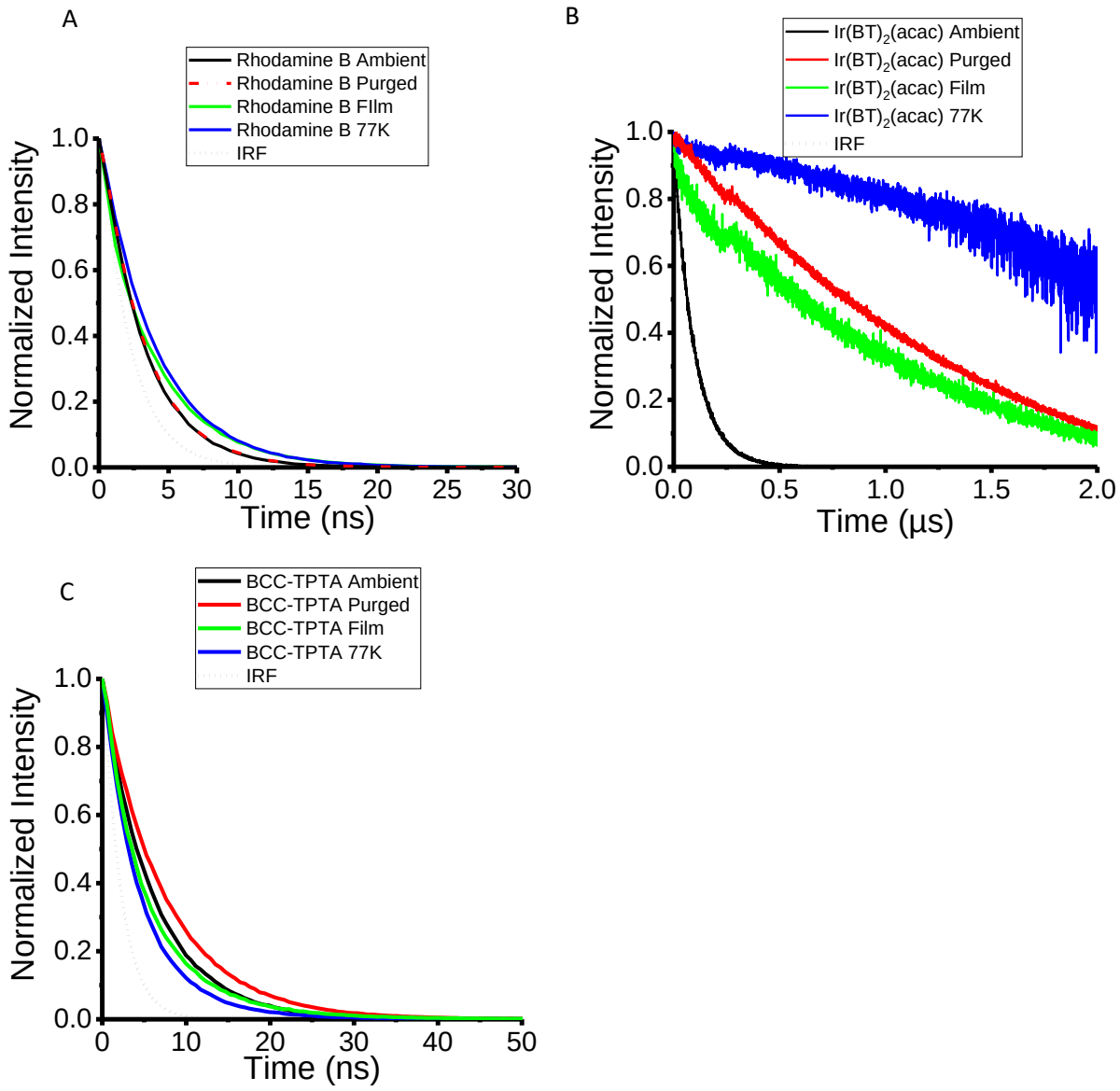

Figure 2. The emissive lifetime of the chromophores was investigated by using the Time Correlated Single Photon Counting (TCSPC) technique: (A) Rhodamine B, (B) $Ir(BT)_2(acac)$, and (C) BCC-TPTA. Measurements were taken at different temperatures and matrixes.

3.3 Time-Resolved Emissive Lifetime Measurements. The time-correlated single photon counting (TCSPC) technique were carried out to evaluate the emissive lifetime from the *ns* to the *µs* timescales of the investigated chromophores. Measurements were done before and after the oxygen purging process, at low temperature (77 K), and in doped film and are shown in ***Figure 2***

while the data is summarized in ***Table 2***. In ***Figure 2A***, the fluorescence decay profile for the Rhodamine B chromophore at ambient conditions can be observed. The decay profiles were obtained with a 400 nm excitation and emission detection at 575 nm. A mono-exponential fit to the decay profile illustrates the 2.92 *ns* relaxation time. This relaxation time matches previously reported fluorescence lifetimes of Rhodamine B in the literature.[40] Also shown in ***Figure 2A*** is the result of purging the solution of oxygen. As can be observed, the oxygen removal has no effect on the fluorescence decay profile of Rhodamine B. A longer fluorescence lifetime at low temperature and in film was obtained for Rhodamine B. This lengthening in the fluorescence lifetime of xanthene derivatives at low temperatures and in PMMA matrixes has been previously documented and can be ascribed to the lack of energy dissipation via chromophore-solvent interaction and by the massive molecular motion suppression induced by the PMMA matrix, respectivly.[49–51]

Table 2. Summary of the emissive lifetime measurements of the investigated chromophores.

Chromophores	Emissive lifetime (Ambient)	Emissive lifetime (Purged)	Emissive lifetime (77K)	Emissive lifetime (Film)
Rhodamine B	2.92 *ns*	2.96 *ns*	3.97 *ns*	3.78 *ns*
Ir(BT)$_2$(acac)	97 *ns*	1.62 μs	4 μs	1.25 μs
BCC-TPTA	6.4 *ns*	7.8 *ns*	4.66 *ns*	5.47 *ns*

These measurements were taken with the Time-Correlated Single Photon Counting (TCSPC) technique.

Shown in ***Figure 2B*** are the emissive characteristics of the Ir(BT)$_2$(acac) complex excited at 400 nm and the emission was detected at 560 nm. The phosphorescence decay profiles for the Ir(BT)$_2$(acac) complex at RT could be fitted to a mono-exponential expression, with a decay time of 97 *ns*. Also notable in ***Figure 2B*** is the decay profile of emission after purging oxygen from the Ir(BT)$_2$(acac) solution. As can be seen from the curve, the decay is drastically lengthened and a mono-exponential expression yielded a phosphorescence lifetime of 1.62 μs. This lengthening in

the phosphorescence lifetime of $Ir(BT)_2(acac)$ explains its $\boldsymbol{\Phi}$ enhancement after the oxygen purging process. This value is in agreement with reported values by Lamansky and others.[41] For such materials with a heavy metal atom in the core, the intersystem crossing (ISC) is expected to be on the order of *ps*.[11,43]

Also shown in ***Figure 2B*** is the phosphorescence lifetime of the $Ir(BT)_2(acac)$ complex at low temperature and in film. As can also be observed, the phosphorescence lifetime of the $Ir(BT)_2(acac)$ complex is drastically lengthened at low temperature (4 μs) and in film (1.25 μs). Sajoto and others have previously documented this lengthening in the phosphorescence lifetime at low temperatures for similar iridium-based complex, and it has been attributed to the lack of thermally activated non-radiative decay channels at low temperatures.[52] Kwon and others have reported a lengthening in the phosphorescence lifetime in chromophores when they are doped into PMMA films, which has been ascribed to the suppression of molecular motions induced by the PMMA matrix.[49]

Shown in ***Figure 2C*** are the emissive dynamics for the BCC-TPTA chromophore. The decay profiles were obtained with 400 nm excitation and 450 nm emission detection wavelength. As can be seen from the curve, a mono-exponential fluorescence decay on the order of 6.4 *ns* was detected at ambient conditions which corresponds well to a singlet (S_1) decay profile. The decay of 6.4 *ns* suggests a relatively efficient fluorescence process in BCC-TPTA. Also noted in ***Figure 2C*** is the result of the oxygen quenching experiment with the BCC-TPTA chromophore. One observes a slightly longer fluorescence decay (7.8 *ns*) after the removal of oxygen from the solution. Interestingly, no long-lived emissive lifetime in the μs region was detected for BCC-TPTA after the oxygen purging process (***Figure 2C*** and ***Figure S10***). This was also true in all the solvents in which the emissive lifetime of BCC-TPTA was investigated (***Figure S6***, ***Table S1***). The emissive

lifetime characterization of BCC-TPTA was also probed with the ns TAS technique (***Figure S11***). The decay profiles were obtained with 415 nm excitation and 450 nm emission detection wavelength. Our ns TAS emissive characterization results are in agreement with the ones obtained by the TCSPC technique and no long-lived emission component in the μs timescale was observed. Measurements were conducted up to 5 μs. The lack of a long-lived emissive lifetime is intriguing. For a reported TADF chromophore with $\boldsymbol{\Phi}$ enhancement of ~ 15 % (from 58 % to 67 %) after the oxygen purging, one would expect to observe a long-lived emissive lifetime spanning the μs timescale as evidence of delayed fluorescence.[53]

Also shown in ***Figure 2C*** is the emissive lifetime of BCC-TPTA at 77 K (4.66 *ns*) and in film (5.47 *ns*). In both cases, a shorter fluorescence lifetime was obtained for BCC-TPTA relative to the ones taken in solution. However, the phosphorescence spectrum of BCC-TPTA taken at 77 K suggests triplet emission at detection wavelengths higher than 470 nm (***Figure S2***). We detected a long-lived emissive component for BCC-TPTA at 77 K when the emission lifetime characterization was conducted at detection wavelengths > 470 nm (***Figure S5***). This long-lived emission component vanished when the temperature was raised and no long-lived emission component was detected at any other temperatures tested (***Figure S4*** and ***Figure S5***). Consequently, this long-lived emissive component at 77 K is attributed to the phosphorescence shown in ***Figure S2***. Interestingly, we did not observe a long-lived emissive lifetime at the μs timescale in film (***Figure 2C*** and ***Figure S10***). A previous study reported a long-lived photoluminescence decay for BCC-TPTA in blended film. This long-lived emissive lifetime was ascribed to a delayed fluorescence process owing to the excited state dynamics of BCC-TPTA.[2] We did not observe long-lived emissive lifetimes indicative of a delayed fluorescence process for

BCC-TPTA at any of the medium tested. Therefore, further spectroscopic techniques were used to characterize the excited state dynamics of BCC-TPTA.

The fluorescence up-conversion (UpC) is a high-time resolution technique with high sensitivity from the *fs* to the *ps* regime.[14] We performed it to evaluate the faster emissive characteristics that could not be investigated by the TCSPC technique. The measurements were done before and after the removal of oxygen from the solution and are shown in ***Figure 3***. The data is summarized in ***Table S3***. In ***Figure 3A***, the fluorescence lifetimes of Rhodamine B before and after oxygen purging can be observed. As expected, there is no effect on the fluorescence lifetime after oxygen purging. In ***Figure 3B***, a rise time in the *ps* regime was observed for the $Ir(BT)_2(acac)$ chromophore. Similar behavior was previously observed for iridium-based phosphorescence chromophores and it was attributed to the ISC process.[43] Interestingly, our data shows that the rise-time is sensitive to O_2. The idea of $[O_2]$ affecting the k_{isc} of chromophores has been suggested.[54] These results illustrate a very long lifetime for $Ir(BT)_2(acac)$.

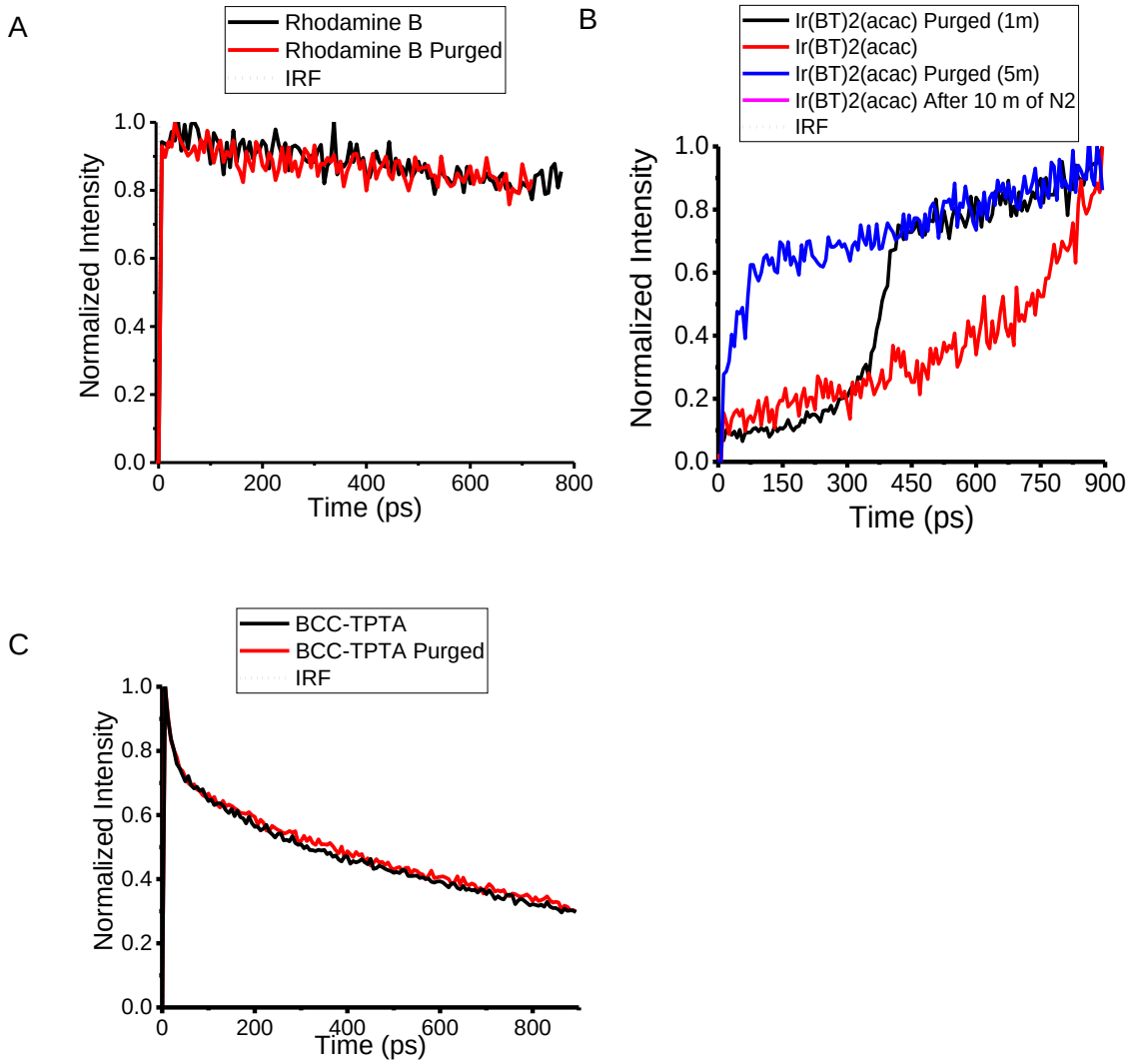

Figure 3. Emissive lifetime of the investigated chromophores probed with the Fluorescence up-conversion technique. All the measurements were done in solution, and before and after the oxygen purging process.

In ***Figure 3C***, the fluorescence lifetime of BCC-TPTA can be observed. In contrast to Rhodamine B, the fluorescence lifetime of BCC-TPTA shows a bi-exponential decay profile. We ascribed this behavior to the donor-acceptor charge transfer nature of BCC-TPTA. Similar multi-exponential behavior has been observed at this timescale in other donor-acceptor chromophores with charger transfer charasteristics.[14,55] The multi-exponential behavior by BCC-TPTA observed

by the UpC also suggests that the lifetime measured by the TCSPC is the second and long component of its fluorescence decay (τ_2). If we compare the UpC of the BCC-TPTA to the $Ir(BT)_2(acac)$ chromophore, the UpC measurements suggest no ISC occurring for BCC-TPTA in the *ps* regime. This was expected. The spin-orbit coupling (SOC) of similar organic chromophores with TADF characteristics are three orders of magnitude smaller than the ones reported for Iridium-based phosphorescence chromophores or copper-based TADF chromophores.[38,41] Given that no evidence of ISC was observed by the UpC, the *ns* TAS was carried out to evaluate if BCC-TPTA possesses triplet transient states that are characteristic of excited stated dynamics governed by a delayed fluorescence mechanism.

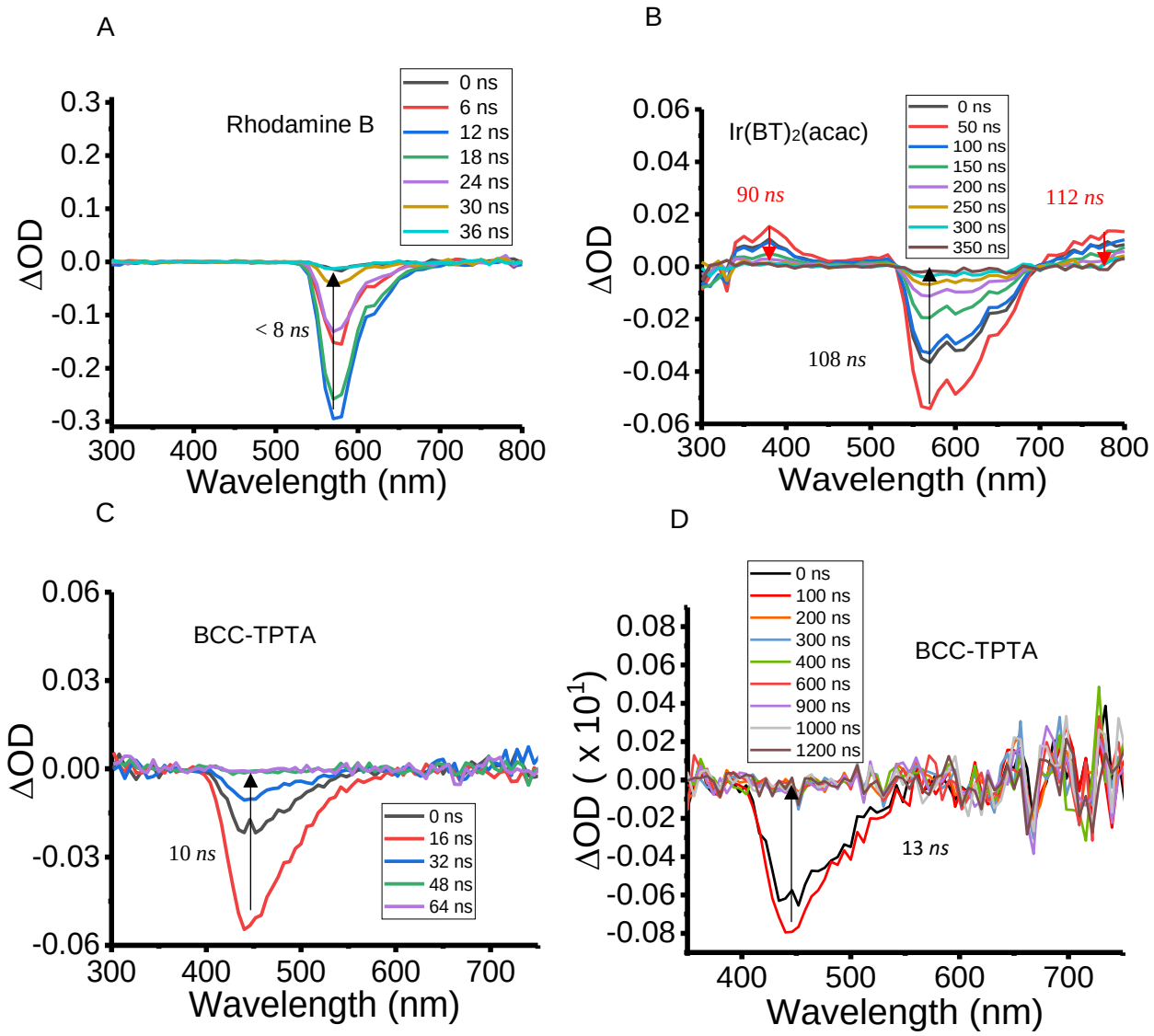

Figure 4. Time-resolved absorption spectra of Rhodamine B (A), $Ir(BT)_2(acac)$ (B), and BCC-TPTA (C), obtained by *ns* TAS. These measurements were conducted in solution and at ambient conditions.

3.4 Nanosecond Transient Absorption Spectroscopy. In order to further investigate the dynamics governing the excited state of BCC-TPTA, the *ns* TAS technique was also done (***Figure 4***), and the data is summarized in ***Table S2***. Our system possesses the ability and sensitivity to see any non-emissive transient states from the *ns* to the *μs* regime.[26,56] In ***Figure 4A***, we observed the

time-resolved absorption spectrum of Rhodamine B in ethanol at ambient conditions. We only obtained one negative optical density (OD) signal from the *ns* TAS measurement. This negative OD band overlaps with the emission spectrum of Rhodamine B (***Figure 1B***). As expected, the kinetic traces of the negative OD band for Rhodamine B correlates well with its fluorescence lifetime obtained by the TCSPC (***Table S2***). Therefore, this negative OD signal is due to the overwhelming fluorescence of Rhodamine B ($S_1 \rightarrow S_0$) detected as has been previously reported.[40] As is typical for fluorescence chromophores, no significant change or evidence of a transient triplet states was observed before or after oxygen purging at the investigated timescales (***Figure S7***).

In ***Figure 4B***, we observed the time-resolved absorption spectrum of the $Ir(BT)_2(acac)$ complex in THF at ambient conditions. For the $Ir(BT)_2(acac)$ complex we detected both, positive (excited state absorption, ESA) and negative OD signals, which is in agreement with previous reported time-resolved absorption spectrums for similar iridium-based chromophores.[57] These transient ESA signals detected by the TAS technique in iridium-based complexes have been previously attributed to spin-forbidden metal-to-ligand charge transfer (MLCT) processes and ligand centered (LC) transitions, which are all related to spin-orbit interactions and singlet to triplet electronic transitions.[43,57] As expected, the kinetic traces obtained from the observed negative OD band correlates well with the $Ir(BT)_2(acac)$ complex phosphorescence lifetime obtained by the TCSPC (***Table S2***). Therefore, this negative OD signal can be attributed to its overwhelming phosphorescence ($T_1 \rightarrow S_0$) detected as has been previously reported for similar iridium-based chromophores.[43,57] The time-resolved absorption spectrum of the $Ir(BT)_2(acac)$ complex and the kinetic traces of its bands before and after the oxygen purging process can be observed in ***Figure S8***. As observed, the time-resolved absorption spectrums of the $Ir(BT)_2(acac)$ complex is highly sensitive to the removal of oxygen. As a result, longer kinetic traces of the time-resolved

absorption bands are obtained after oxygen removal. This sensitivity to oxygen is in agreement with the emissive profile obtained by the TCSPC technique and is indicative of $Ir(BT)_2(acac)$ excited state triplet nature.

In ***Figure 4C*** and ***Figure 4D***, we observed the time-resolved absorption spectra of BCC-TPTA in toluene at ambient conditions for the *ns* and μs timescales, respectively. Interestingly, we detected only one signal as a negative OD band for BCC-TPTA at any of the investigated timescales. This band perfectly overlaps with the emission spectrum of BCC-TPTA. In addition, its kinetic trace correlates well with the fluorescence lifetime obtained by the TCSPC (***Table S2***). Therefore, as with the Rhodamine B, the only signal obtained for BCC-TPTA is attributed to its overwhelming fluorescence ($S_1 \rightarrow S_0$) detected. No significant effect in the time-resolved absorption spectrum of BCC-TPTA was observed after the removal of oxygen from the solution at any of the investigated timescales (***Figure S9***). This was intriguing. Given the 15% (58 % to 67 %) $\boldsymbol{\Phi}$ enhancement after the removal of oxygen from the solution, we expected to see triplet transient signals in the form of ESA bands for BCC-TPTA. These ESA bands should be observed from the *ns* to the μs timescale, as it has been documented in similar organic chromophores with TADF characteristics.[53]

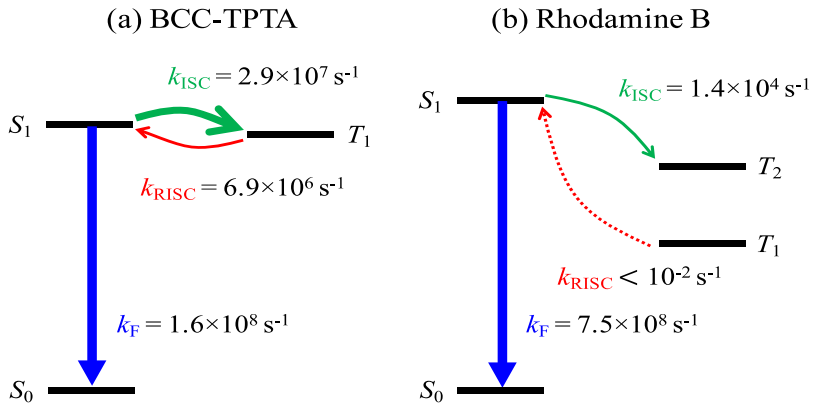

Figure 5. Energy diagram of the fluorescence, intersystem crossing, and reverse intersystem crossing rates for (a) BCC-TPTA and (b) Rhodamine B.

Table 3. Calculated rate constants of fluorescence (k_F), ISC (k_{ISC}), and rISC (k_{rISC}), and available experimental values. (The ratio of the quantity to k_F is given in the parenthesis)

Dynamic Process	BCC-TPTA			Rhodamine B		
	Calc k (s^{-1})	Calc τ (ns)	Expt.[2]	Calc k (s^{-1})	Calc τ (ns)	Expt.[58]
Fluorescence	1.6×10^{8} (1.00)	6	9.6×10^{7}	7.5×10^{8} (1.00)	1	N/A
ISC	2.9×10^{7} (0.18)	34	4.2×10^{7}	1.4×10^{4} (1.9×10^{-5})	$\sim 10^{5}$	5.3×10^{5}
RISC	6.9×10^{6} (0.04)	146	N/A	< 0.01 (10^{-11})	$> 10^{11}$	N/A

3.5 Quantum Chemical Simulations. Quantum chemical simulations (QCS) were carried out to gain a deeper understanding of the key differences between BCC-TPTA and Rhodamine B. Specifically, the rate of fluorescence (k_F), the rate of intersystem crossing (k_{ISC}), and the rate of reverse intersystem crossing (k_{rISC}) of these chromophores were determined by using a Fermi-Golden rule rate based on spin-orbital couplings from time-dependent density functional theory and are reported in ***Table 3***.[32,59] BCC-TPTA has k_{ISC} and k_{rISC} values that are significantly larger than those for Rhodamine B, and these are comparable with the rate constant for fluorescence decay. The large k_{ISC} and k_{rISC} of BCC-TPTA originated from small ΔE_{ST} (0.34 eV) and indicate

efficient population transfer between singlet and triplet, which is a distinct property of BCC-TPTA. On the other hand, for Rhodamine B, a typical fluorescent chromophore, the relevant rate constants follow the pattern: $k_F >> k_{ISC} >> k_{rISC}$. The k_F of Rhodamine B is four orders of magnitude larger than its k_{ISC} and ten orders of magnitude larger than its k_{rISC}. For BCC-TPTA chromophore, the calculated rate constants suggest that the fluorescence, ISC, and rISC processes all occur on a *ns* timescale. With these findings, it is suggested that this system exhibits a dynamic equilibrium between the k_f, the k_{ISC}, and the k_{rISC}, which is important for a delayed fluorescence process.

4. DISCUSSION

In this study, we used high-time resolution ultrafast spectroscopy, with an emphasis on the *ns* TAS, to probe the excited state dynamic of a TADF chromophores with a reported η_{IQE} of 84 %.[2] Also, two well-known fluorescence and phosphorescence standards, Rhodamine B and $Ir(BT)_2(acac)$, respectively, were used for comparison. The steady state measurements showed optical activity in the UV-Vis region for all the investigated chromophores. The $\boldsymbol{\Phi}$ measurements showed that BCC-TPTA has a higher sensitivity to oxygen than Rhodamine B but not as much sensitivity as the $Ir(BT)_2(acac)$ complex. This BCC-TPTA sensitivity to oxygen was observed as an enhancement in the $\boldsymbol{\Phi}$ after the removal of oxygen from the solution, and has been ascribed due to a delayed fluorescence process happening in the μs timescale.[2,6,11,38,60,61] This delayed fluorescence process implies multiple electronic transitions in the excited states that are quantum mechanically forbidden. The probability of these transitions happening has been ascribed to the nature of their spin-orbit coupling (SOC), their small exchange energy (ΔE_{st}), and the existence of locally excited triplet state (^{3}LE).[38,53] Therefore, several ultrafast spectroscopic techniques were coupled with QCS to evaluate the excited state dynamics governing in BCC-TPTA.

Our emissive lifetime characterization measurements showed a lengthening in the fluorescence lifetime for BCC-TPTA after the removal of oxygen, which correlates well with its ***Φ*** enhancement. However, this lengthening was only about ~ 2 *ns* and no evidence of a long-lived emissive lifetime characteristic from a chromophore with excited state dynamics governed by a TADF mechanism was observed by any our spectroscopic tools (***Figure 2C, Figure S6, Figure S10, and Figure S11***). Literature shows extensive evidence of studies trying to understand the molecular oxygen quenching mechanism in a repertoire of organic chromophores with similar fluorescence lifetimes to the ones reported in this study.[12,62] Those studies have highlighted the fluorescence (S_1) sensitivity to oxygen even at ambient conditions.[62] The Stern-Volmer equation was used to evaluate the quenching mechanism in which oxygen affects the excited state dynamics of the investigated chromophores. This equation would help us to calculate the emissive quenching rates of the investigated chromophores. After solving the equation (***Table 1***), it showed that the quenching rate constant for BCC-TPTA in toluene is about the oxygen diffusion limit in toluene.[62] This implies that oxygen can significantly quench the fluorescence (S_1) of BCC-TPTA via a collisional mechanism. This explains the lengthening in the fluorescence lifetime and the ***Φ*** enhancement of BCC-TPTA after the removal of oxygen from the solution. This oxygen quenching effect was not observed for Rhodamine B. This is due to its significantly faster fluorescence lifetime compared to the ones obtained for BCC-TPTA. In the case of the $Ir(BT)_2(acac)$ complex, it is well known that the robust lengthening in the phosphorescence lifetime after the removal of oxygen is due to the triplet emissive nature of its excited state.[41,62] In addition, the fluorescence UpC measurements suggests that the emission detected by the TCSPC comes from BCC-TPTA second and long component of its fluorescence decay (***Figure 3C***). The comprehensive study on the emissive lifetimes obtained from the UpC and the TCSPC techniques

suggests that BCC-TPTA have emissive dynamics as that of a typical fluorescence chromophore with charge transfer nature.

Studies have highlighted the effect of the dielectric constant of the medium and polarity of the solvent on the ΔE_{st} of molecules with TADF character.[63,64] Therefore, we probed the emissive lifetime of BCC-TPTA in different solvents to evaluate if the long-lived emissive lifetime was characteristic of a particular environment. As can be observed in ***Figure S6***, no long-lived emissive lifetime was obtained in any of the solvents tested. In ***Table S1***, we observed a proportional relationship between the fluorescence lifetime of BCC-TPTA and the solvent polarity in which the measurement was done. When we conducted the emissive lifetime characterization of BCC-TPTA at 77 K, we thought that the low temperature would prevent energy dissipation via non-radiative pathways, which should result in a longer fluorescence lifetime. Interestingly, we observed a faster fluorescence lifetime at 77 K relative to the one taken at RT. We also detected a long-lived phosphorescence emission for BCC-TPTA at detection wavelengths > 470 nm. This long-lived emissive component vanished when the temperature was raised (***Figure S4*** and ***Figure S5***). These observations highlighted the lack of a long-lived emissive components for BCC-TPTA at higher temperatures than 77 K. This lack of a long-lived emissive component at high temperatures is not consistent with excited state dynamics governed by a TADF mechanism.[2,6,9,53] In ***Figure S3***, the fluorescence spectra at 77 K showed a blue-shift relative to the one taken at RT. A blue-shift in the emission spectra and faster fluorescence lifetimes in film relative to the one taken in solution were also observed for BCC-TPTA (***Figure S13***). In all cases, a lower energy in the emission spectra of BCC-TPTA was correlated with a longer fluorescence lifetime.[63,64] These results shows the effect of the medium on the S_1 stabilization of BCC-TPTA, which implies that the molecular

conformation of BCC-TPTA is highly dependent on the medium. Yet, no evidence of a long-lived emissive lifetime for BCC-TPTA was observed at RT in any of the medium tested.

We would like to reiterate that we did not observe any long-lived emissive lifetime spanning the μs timescale for BCC-TPTA at any of the conditions tested with any of our spectroscopic tools. This lack of long-lived emissive lifetime was intriguing. A previous study reported a long-lived emissive lifetime in the μs timescale for BCC-TPTA in blended film, which was ascribed to a delayed fluorescence process owing to the excited state properties of BCC-TPTA.[2] We noticed that the emissive decay reported in solid state was conducted by using bis[2-(diphenylphosphino)phenyl] ether oxide (DPEPO) as the host material. The problem with using DPEPO as the host material is that it has steady-state optical properties in the same range of wavelengths that BCC-TPTA does.[2,21,65] Furthermore, emissive lifetime in the μs timescale has been reported for DPEPO and its derivatives.[21] This overlap in the steady-state optical properties and the long-lived emissive character of DPEPO could give rise to excited state mechanisms such as FRET transfer and DET among the chromophores.[2,21,65] In contrast to the electroluminescence process, the excited state and bandgap optimization between the guest:host is detrimental for the photoluminescence process. This is due to the ambitious nature of deconvoluting and quantifying the influence of the host in the obtained emissive properties of the film.[65–67] In this study, the selection of an optically inert host such as PMMA showed that BCC-TPTA seems to have emissive lifetimes characteristics of a fluorescence chromophore.

We carried out the *ns* TAS technique to further investigate and compare the excited state dynamics of the investigated chromophores. Correctly, we were probing for triplet transient state signals that could be linked to a delayed fluorescence mechanism in BCC-TPTA. Previous studies have reported transient absorption measurements for similar organic chromophores with TADF

characteristics.[15,53,68] Specifically, they have reported ESA between 500-700 nm in blue and light-blue TADF chromophores.[53,68] This ESA has been linked to the ^{3}LE state, which is believed to be an integral state for the rISC facilitation.[38,53] Interestingly, the time-resolved absorption spectrum of BCC-TPTA behaves similar to the one obtained for Rhodamine B and no ESA was detected by the *ns* TAS techniques at any of the investigated timescales. Long-lived ESA was observed for the $Ir(BT)_2(acac)$ complex at the investigated timescales. These transient species detected on the $Ir(BT)_2(acac)$ complex have been linked to MLCT and LC transitions, which are all related to spin-forbidden electronic transitions.[43,57] In contrast to the ESA observed for the $Ir(BT)_2(acac)$ complex and with similar *ns* TAS conducted in similar organic chromophores with TADF characteristic, no evidence of the ^{3}LE state nor any triplet transient state at all was observed for BCC-TPTA. Studies conducted in similar organic chromophores with TADF characteristics have been able to correlate the presence of this ^{3}LE state with their observable long-lived μs emissive lifetimes after photoexcitation.[15,53] Furthermore, Kuang et al reported the detection of robust long-lived triplet transient states in chromophores with TADF characteristics despite of their limited long-lived emissive profile in solution.[68] Still, that study highlighted the transient triplet state as the focal point of the TADF mechanism.[53,68] Despite our quantum chemical simulations suggesting a dynamic equilibrium between the k_F, the k_{ISC}, and the k_{rISC} in the *ns* timescale for BCC-TPTA, our transient absorption experiments are highlighted by the lack of the ^{3}LE state or any triplet transient state. This lack of the ^{3}LE state could also explains why we do not observe long-lived emissive lifetime at in any of the medium tested by our multiple spectroscopic tools. Herein, the experimental evidence presented in this report suggests that BCC-TPTA has excited state dynamics of a typical fluorescence chromophore. As a result, we believe the influence of the electronic and optical properties of the host materials has been overlooked in previous studies

intended to report the photophysical properties of organic chromophores with TADF characteristics.

5. CONCLUSIONS

Herein, we report the first study in which multiple time-resolved spectroscopic techniques, with an emphasis in the *ns* TAS, were coupled with QCS to elucidate the excited state dynamics of a reported chromophore (BCC-TPTA) with highly efficient blue TADF characteristics. We carried out a comparison of this chromophore with two well-known fluorescent and phosphorescent chromophores. The BCC-TPTA chromophore showed some sensitivity to the removal of oxygen but not as strong as the phosphorescent $Ir(BT)_2(acac)$ chromophore and not as small as the fluorescent Rhodamine B chromophore. The sensitivity to oxygen from BCC-TPTA was observed as an enhancement in the $\boldsymbol{\Phi}$ after purging oxygen from the solution, which has been previously attributed to a delayed fluorescence process occurring in the μs timescale.[2] The evidence obtained by our spectroscopic tools showed that: (1) BCC-TPTA does not have a long-lived emissive lifetime that could be linked to a delayed fluorescence mechanism in any of the medium tested; (2) BCC-TPTA does not have any triplet transient state that could be linked to an excited state dynamic governed by a delayed fluorescence process. Therefore, the $\boldsymbol{\Phi}$ enhancement of BCC-TPTA after the oxygen purging process is ascribed to the lack of oxygen-collisional quenching of the fluorescence (S_1) rather than due to a delayed fluorescence process. These results imply that just comparing the $\boldsymbol{\Phi}$ difference before and after purging oxygen from the solution is not an accurate method to claim excited state dynamics governed by a delayed fluorescence mechanism. Consequently, the development of a better and more accurate method with a focus in probing and

characterizing the triplet state is in need. We believed that the *ns* TAS technique should be integral in the triplet characterization of rational designed chromophores with TADF characteristics.

Despite that the phosphorescence spectrum measurements on BCC-TPTA may have showed hints of a small ΔE_{ST}, our study suggests that BCC-TPTA has excited state dynamics such as typical fluorescence chromophores. Furthermore, this study suggests that previous studies in which the optical properties of organic chromophores with TADF characteristics are reported may have overlooked the influence and impact of the host electronic transitions on the obtained optical properties.

Conflicts of interest

There are no conflicts to declare.

Acknowledgments

TGIII acknowledges support by the U.S.A. Department of Energy, Office of Energy, Office of Basic Energy Science, Photochemistry, via Grant (DE-SC0012482).

REFERENCES

1 M. Hong, M. K. Ravva, P. Winget and J. L. Brédas, *Chem. Mater.*, 2016, **28**, 5791–5798.

2 S. Hirata, Y. Sakai, K. Masui, H. Tanaka, S. Y. Lee, H. Nomura, N. Nakamura, M. Yasumatsu, H. Nakanotani, Q. Zhang, K. Shizu, H. Miyazaki and C. Adachi, *Nat. Mater.*, 2015, **14**, 330–336.

3 F. B. Dias, K. N. Bourdakos, V. Jankus, K. C. Moss, K. T. Kamtekar, V. Bhalla, J. Santos, M. R. Bryce and A. P. Monkman, *Adv. Mater.*, 2013, **25**, 3707–14.

4 H. Nakanotani, K. Masui, J. Nishide, T. Shibata and C. Adachi, *Sci. Rep.*, 2013, **3**, 2127.

5 Y. J. Shiu, Y. C. Cheng, W. L. Tsai, C. C. Wu, C. T. Chao, C. W. Lu, Y. Chi, Y. T. Chen, S. H. Liu and P. T. Chou, *Angew. Chemie - Int. Ed.*, 2016, **55**, 3017–3021.

6 Y. Tao, K. Yuan, T. Chen, P. Xu, H. Li, R. Chen, C. Zheng, L. Zhang and W. Huang, *Adv. Mater.*, 2014, **26**, 7931–58.

7 H. Kaji, H. Suzuki, T. Fukushima, K. Shizu, K. Suzuki, S. Kubo, T. Komino, H. Oiwa, F. Suzuki, A. Wakamiya, Y. Murata and C. Adachi, *Nat. Commun.*, 2015, **6**, 8476.

8 S. Youn Lee, T. Yasuda, H. Nomura and C. Adachi, *Appl. Phys. Lett.*, 2012, **101**, 093306.

9 H. Uoyama, K. Goushi, K. Shizu, H. Nomura and C. Adachi, *Nature*, 2012, **492**, 234–238.

10 A. Endo, M. Ogasawara, A. Takahashi, D. Yokoyama, Y. Kato and C. Adachi, *Adv. Mater.*, 2009, **21**, 4802–6.

11 L. Bergmann, G. J. Hedley, T. Baumann, S. Bräse and I. D. W. Samuel, *Sci. Adv.* 2016, **2**, DOI:10.1126/sciadv.1500889.

12 F. Wilkinson and A. A. Abdel-Shafi, *J. Phys. Chem. A*, 1997, **101**, 5509–5516.

13 C. Grewer and H. D. Brauer, *J. Phys. Chem.*, 1994, **98**, 4230–4235.

14 R. J. Vázquez, H. Kim, B. M. Kobilka, B. J. Hale, M. Jeffries-El, P. Zimmerman and T. Goodson, *J. Phys. Chem. C*, 2017, **121**, 14382–14392.

15 Z. Yang, Z. Mao, Z. Xie, Y. Zhang, S. Liu, J. Zhao, J. Xu, Z. Chi and M. P. Aldred, *Chem. Soc. Rev.*, 2017, **46**, 915–1016.

16 P. L. Dos Santos, J. S. Ward, M. R. Bryce and A. P. Monkman, *J. Phys. Chem. Lett.*, 2016, **7**, 3341–3346.

17 J. B. Birks, *Nature*, 1967, **214**, 1187–1190.

18 D. H. Kim, A. D'Aléo, X. K. Chen, A. D. S. Sandanayaka, D. Yao, L. Zhao, T. Komino, E. Zaborova, G. Canard, Y. Tsuchiya, E. Choi, J. W. Wu, F. Fages, J. L. Brédas, J. C. Ribierre and C. Adachi, *Nat. Photonics*, 2018, **12**, 98–104.

19 X.-K. Chen, Y. Tsuchiya, Y. Ishikawa, C. Zhong, C. Adachi and J.-L. Brédas, *Adv. Mater.*, 2017, **29**, 1702767.

20 H. M. Zidan and M. Abu-Elnader, *Phys. B Condens. Matter*, 2005, **355**, 308–317.

21 J. Zhang, D. Ding, Y. Wei, F. Han, H. Xu and W. Huang, *Adv. Mater.*, 2016, **28**, 479–485.

22 G. Jones, W. R. Jackson, C. Y. Choi and W. R. Bergmark, *J. Phys. Chem.*, 1985, **89**, 294–300.

23 R. F. Kubin and A. N. Fletcher, *J. Lumin.*, 1982, **27**, 455–462.

24 B. Keller, A. McLean, B. G. Kim, K. Chung, J. Kim and T. Goodson, *J. Phys. Chem. C*, 2016, **120**, 9088–9096.

25 O. Varnavski, T. Goodson, L. Sukhomlinova and R. Twieg, *J. Phys. Chem. B*, 2004, **108**, 10484–10492.

26 H. Kim, B. Keller, R. Ho-Wu, N. Abeyasinghe, R. J. Vázquez, T. Goodson and P. M. Zimmerman, *J. Am. Chem. Soc.*, 2018, **140**, 7760–7763.

27 T. Kowalczyk, T. Tsuchimochi, P. T. Chen, L. Top and T. Van Voorhis, *J. Chem. Phys.*, 2013, **138**, 164101.

28 D. Hait, T. Zhu, D. P. McMahon and T. Van Voorhis, *J. Chem. Theory Comput.*, 2016, **12**, 3353–3359.

29 I. Frank, J. Hutter, D. Marx and M. Parrinello, *J. Chem. Phys.*, 1998, **108**, 4060–4069.

30 I. Okazaki, F. Sato, T. Yoshihiro, T. Ueno and H. Kashiwagi, *J. Mol. Struct. THEOCHEM*, 1998, **451**, 109–119.

31 M. Filatov and S. Shaik, *Chem. Phys. Lett.*, 1999, **304**, 429–437.

32 Y. Shao, Z. Gan, E. Epifanovsky, A. T. B. Gilbert, M. Wormit, J. Kussmann, A. W. Lange, A. Behn, J. Deng, X. Feng, D. Ghosh, M. Goldey, P. R. Horn, L. D. Jacobson, I. Kaliman, R. Z. Khaliullin, T. Kuś, A. Landau, J. Liu, E. I. Proynov, Y. M. Rhee, R. M. Richard, M. A. Rohrdanz, R. P. Steele, E. J. Sundstrom, H. L. Woodcock, P. M. Zimmerman, D. Zuev, B. Albrecht, E. Alguire, B. Austin, G. J. O. O. Beran, Y. A. Bernard, E. Berquist, K. Brandhorst, K. B. Bravaya, S. T. Brown, D. Casanova, C.-M. M. Chang, Y. Chen, S. H. Chien, K. D. Closser, D. L. Crittenden, M. Diedenhofen, R. A. Distasio, H. Do, A. D. Dutoi, R. G. Edgar, S. Fatehi, L. Fusti-Molnar, A. Ghysels, A. Golubeva-Zadorozhnaya, J. Gomes, M. W. D. Hanson-Heine, P. H. P. Harbach, A. W. Hauser, E. G. Hohenstein, Z. C. Holden, T.-C. C. Jagau, H. Ji, B. Kaduk, K. Khistyaev, J. J. Kim, J. J. Kim, R. A. King, P. Klunzinger, D. Kosenkov, T. Kowalczyk, C. M. Krauter, K. U. Lao, A. D. Laurent, K. V. Lawler, S. V. Levchenko, C. Y. Lin, F. Liu, E. Livshits, R. C. Lochan, A. Luenser, P. Manohar, S. F. Manzer, S.-P. P. Mao, N. Mardirossian, A. V. Marenich, S. A. Maurer, N. J. Mayhall, E. Neuscamman, C. M. Oana, R. Olivares-Amaya, D. P. O'Neill, J. A. Parkhill, T. M. Perrine, R. Peverati, A. Prociuk, D. R. Rehn, E. Rosta, N. J. Russ, S. M. Sharada, S. Sharma, D. W. Small, A. Sodt, T. Stein, D. Stück, Y.-C. C. Su, A. J. W. Thom, T. Tsuchimochi, V. Vanovschi, L. Vogt, O. Vydrov, T. Wang, M. A. Watson, J. Wenzel, A. White, C. F. Williams, J. Yang, S. Yeganeh, S. R. Yost, Z.-Q. Q. You, I. Y. Zhang, X. Zhang, Y. Zhao, B. R. Brooks, G. K. L. Chan, D. M. Chipman, C. J. Cramer, W. A. Goddard, M. S. Gordon, W. J. Hehre, A. Klamt, H. F. Schaefer, M. W. Schmidt, C. D. Sherrill, D. G. Truhlar, A. Warshel, X. Xu, A. Aspuru-Guzik, R. Baer, A. T. Bell, N. A. Besley, J.-D. Da Chai, A. Dreuw, B. D. Dunietz, T. R. Furlani, S. R. Gwaltney, C.-P. P.

Hsu, Y. Jung, J. Kong, D. S. Lambrecht, W. Liang, C. Ochsenfeld, V. A. Rassolov, L. V. Slipchenko, J. E. Subotnik, T. Van Voorhis, J. M. Herbert, A. I. Krylov, P. M. W. Gill, M. Head-Gordon, T. Kuš, A. Landau, J. Liu, E. I. Proynov, Y. M. Rhee, R. M. Richard, M. A. Rohrdanz, R. P. Steele, E. J. Sundstrom, H. L. Woodcock, P. M. Zimmerman, D. Zuev, B. Albrecht, E. Alguire, B. Austin, G. J. O. O. Beran, Y. A. Bernard, E. Berquist, K. Brandhorst, K. B. Bravaya, S. T. Brown, D. Casanova, C.-M. M. Chang, Y. Chen, S. H. Chien, K. D. Closser, D. L. Crittenden, M. Diedenhofen, R. A. Distasio, H. Do, A. D. Dutoi, R. G. Edgar, S. Fatehi, L. Fusti-Molnar, A. Ghysels, A. Golubeva-Zadorozhnaya, J. Gomes, M. W. D. Hanson-Heine, P. H. P. Harbach, A. W. Hauser, E. G. Hohenstein, Z. C. Holden, T.-C. C. Jagau, H. Ji, B. Kaduk, K. Khistyaev, J. J. Kim, J. J. Kim, R. A. King, P. Klunzinger, D. Kosenkov, T. Kowalczyk, C. M. Krauter, K. U. Lao, A. D. Laurent, K. V. Lawler, S. V. Levchenko, C. Y. Lin, F. Liu, E. Livshits, R. C. Lochan, A. Luenser, P. Manohar, S. F. Manzer, S.-P. P. Mao, N. Mardirossian, A. V. Marenich, S. A. Maurer, N. J. Mayhall, E. Neuscamman, C. M. Oana, R. Olivares-Amaya, D. P. Oneill, J. A. Parkhill, T. M. Perrine, R. Peverati, A. Prociuk, D. R. Rehn, E. Rosta, N. J. Russ, S. M. Sharada, S. Sharma, D. W. Small, A. Sodt, T. Stein, D. Stück, Y.-C. C. Su, A. J. W. Thom, T. Tsuchimochi, V. Vanovschi, L. Vogt, O. Vydrov, T. Wang, M. A. Watson, J. Wenzel, A. White, C. F. Williams, J. Yang, S. Yeganeh, S. R. Yost, Z.-Q. Q. You, I. Y. Zhang, X. Zhang, Y. Zhao, B. R. Brooks, G. K. L. Chan, D. M. Chipman, C. J. Cramer, W. A. Goddard, M. S. Gordon, W. J. Hehre, A. Klamt, H. F. Schaefer, M. W. Schmidt, C. D. Sherrill, D. G. Truhlar, A. Warshel, X. Xu, A. Aspuru-Guzik, R. Baer, A. T. Bell, N. A. Besley, J.-D. Da Chai, A. Dreuw, B. D. Dunietz, T. R. Furlani, S. R. Gwaltney, C.-P. P. Hsu, Y. Jung, J. Kong, D. S. Lambrecht, W. Liang, C. Ochsenfeld, V. A. Rassolov, L. V.

Slipchenko, J. E. Subotnik, T. Van Voorhis, J. M. Herbert, A. I. Krylov, P. M. W. Gill and M. Head-Gordon, *Mol. Phys.*, 2015, **113**, 184–215.

33 G. W. Robinson and R. P. Frosch, *J. Chem. Phys.*, 1963, **38**, 1187–1203.

34 V. Lawetz, G. Orlandi and W. Siebrand, *J. Chem. Phys.*, 1972, **56**, 4058–4072.

35 J. L. Brédas, D. Beljonne, V. Coropceanu and J. Cornil, *Chem. Rev.*, 2004, **104**, 4971–5003.

36 K. Schmidt, S. Brovelli, V. Coropceanu, D. Beljonne, J. Cornil, C. Bazzini, T. Caronna, R. Tubino, F. Meinardi, Z. Shuai and J. L. Brédas, *J. Phys. Chem. A*, 2007, **111**, 10490–10499.

37 D. Beljonne, Z. Shuai, G. Pourtois and J. L. Bredas, *J. Phys. Chem. A*, 2001, **105**, 3899–3907.

38 P. K. Samanta, D. Kim, V. Coropceanu and J. L. Brédas, *J. Am. Chem. Soc.*, 2017, **139**, 4042–4051.

39 Q. Zhang, H. Kuwabara, W. J. Potscavage, S. Huang, Y. Hatae, T. Shibata and C. Adachi, *J. Am. Chem. Soc.*, 2014, **136**, 18070–18081.

40 P. C. Beaumont, D. G. Johnson and B. J. Parsons, *J. Chem. Soc. Faraday Trans.*, 1993, **89**, 4185–4191.

41 S. Lamansky, P. Djurovich, D. Murphy, F. Abdel-Razzaq, R. Kwong, I. Tsyba, M. Bortz, B. Mui, R. Bau and M. E. Thompson, *Inorg. Chem.*, 2001, **40**, 1704–1711.

42 P. H. Doan, D. R. G. Pitter, A. Kocher, J. N. Wilson and T. Goodson, *J. Am. Chem. Soc.*, 2015, **137**, 9198–9201.

43 K. C. Tang, K. L. Liu and I. C. Chen, *Chem. Phys. Lett.*, 2004, **386**, 437–441.

44 C. Han, Z. Zhang, D. Ding and H. Xu, *Chem*, 2018, **4**, 2154–2167.

45 W. Li, D. Liu, F. Shen, D. Ma, Z. Wang, T. Feng, Y. Xu, B. Yang and Y. Ma, *Adv. Funct. Mater.*, 2012, **22**, 2797–2803.

46 R. W. Chambers, T. Kajiwara and D. R. Kearns, *J. Phys. Chem.*, 1974, **78**, 380–387.

47 C. Adachi, M. A. Baldo, S. R. Forrest, S. Lamansky, M. E. Thompson and R. C. Kwong, *Appl. Phys. Lett.*, 2001, **78**, 1622–1624.

48 M. A. Baldo, S. Lamansky, P. E. Burrows, M. E. Thompson and S. R. Forrest, *Appl. Phys. Lett.*, 1999, **75**, 4–6.

49 M. S. Kwon, Y. Yu, C. Coburn, A. W. Phillips, K. Chung, A. Shanker, J. Jung, G. Kim, K. Pipe, S. R. Forrest, J. H. Youk, J. Gierschner and J. Kim, *Nat. Commun.* 2015, **6**, DOI:10.1038/ncomms9947.

50 T. J. V. Prazeres, A. Fedorov, S. P. Barbosa, J. M. G. Martinho and M. N. Berberan-Santos, *J. Phys. Chem. A*, 2008, **112**, 5034–5039.

51 K. Kemnitz, N. Tamai, I. Yamazaki, N. Nakashima and K. Yoshihara, *J. Phys. Chem.*, 1986, **90**, 5094–5101.

52 T. Sajoto, P. I. Djurovich, A. B. Tamayo, J. Oxgaard, W. A. Goddard and M. E. Thompson, *J. Am. Chem. Soc.*, 2009, **131**, 9813–9822.

53 T. Hosokai, H. Matsuzaki, H. Nakanotani, K. Tokumaru, T. Tsutsui, A. Furube, K. Nasu, H. Nomura, M. Yahiro and C. Adachi, *Sci. Adv.* 2017, **5**, DOI:10.1126/sciadv.1603282.

54 A. J. McLean, D. J. McGarvey, T. G. Truscott, C. R. Lambert and E. J. Land, *J. Chem. Soc. Faraday Trans.*, 1990, **86**, 3075.

55 Z. Cai, R. J. Vázquez, D. Zhao, L. Li, W. Y. Lo, N. Zhang, Q. Wu, B. Keller, A. Eshun, N. Abeyasinghe, H. Banaszak-Holl, T. Goodson and L. Yu, *Chem. Mater.*, 2017, **29**, 6726–6732.

56 T. J. Whittemore, T. A. White and C. Turro, *J. Am. Chem. Soc.*, 2018, **140**, 229–234.

57 F. Lafolet, S. Welter, Z. Popović and L. De Cola, *J. Mater. Chem.*, 2005, 15, 2820–2828.

58 R. Menzel and E. Thiel, *Chem. Phys. Lett.*, 1998, **291**, 237–243.

59 L. Visscher, *Theor. Comput. Chem.*, 2002, **11**, 291–331.

60 D. R. Lee, S.-H. Hwang, S. K. Jeon, C. W. Lee and J. Y. Lee, *Chem. Commun.*, 2015, **51**, 8105–8107.

61 T. Hatakeyama, K. Shiren, K. Nakajima, S. Nomura, S. Nakatsuka, K. Kinoshita, J. Ni, Y. Ono and T. Ikuta, *Adv. Mater.*, 2016, **28**, 2777–2781.

62 C. Schweitzer and R. Schmidt, *Chem. Rev.*, 2003, **103**, 1685–1758.

63 R. Ishimatsu, S. Matsunami, K. Shizu, C. Adachi, K. Nakano and T. Imato, *J. Phys. Chem. A*, 2013, **117**, 5607–5612.

64 H. Sun, Z. Hu, C. Zhong, X. Chen, Z. Sun and J. L. Brédas, *J. Phys. Chem. Lett.*, 2017, **8**, 2393–2398.

65 K. E. Sapsford, L. Berti and I. L. Medintz, *Angew. Chemie - Int. Ed.*, 2006, **45**, 4562–4588.

66 P. R. Selvin, *Nat. Struct. Mol. Biol.*, 2000, **7**, 730–734.

67 H. Fukagawa, T. Shimizu, Y. Iwasaki and T. Yamamoto, *Sci. Rep.*, 2017, **7**, 1735.

68 Z. Kuang, G. He, H. Song, X. Wang, Z. Hu, H. Sun, Y. Wan, Q. Guo and A. Xia, *J. Phys. Chem. C*, 2018, **122**, 3727–3737.

Table of Content Graphic